THE OBSERVATION OF SINGLE MOLECULE CROSS-CORRELATION FUNCTIONS USING ELECTRIC FIELD INDUCED BIREFRINGENCE

M.W. EVANS
Department of Physics, U.C.N.W., Bangor, Gwynedd, Wales, UK

Received 20 March 1984

A method is devised for the measurement of basic single molecule cross-correlation functions (ccf's) such as $\langle \mathbf{v}(t)\boldsymbol{\omega}^{\mathrm{T}}(0)\rangle$ or $\langle \mathbf{v}(t)\dot{\boldsymbol{\mu}}^{\mathrm{T}}(0)\rangle$. Here $\mathbf{v}$ is the centre of mass linear velocity, $\boldsymbol{\omega}$ the angular velocity and $\boldsymbol{\mu}$ the dipole moment of the same molecule. The appearance under electric field treatment of these ccf's in the laboratory frame is demonstrated using both computer simulation and analytical theory. They are inevitable consequences of the induction in a molecular liquid of birefringence. Conversely the experimental technique of electric field induced birefringence may be used to measure them directly.

Introduction. It is possible to measure with great accuracy a minute birefringence induced in a molecular liquid. The birefringence may be induced with an electric field, and information obtained in this way about the molecular dynamics of the liquid or liquid crystal states [1]. It is partly the purpose of this letter to show that the theory of electric field induced birefringence is deficient in at least one respect: it ignores the appearance in the laboratory frame of single molecule cross-correlation functions [2–4] (ccf's) exemplified by $\langle \mathbf{v}(t)\boldsymbol{\omega}^{\mathrm{T}}(0)\rangle$ and $\langle \mathbf{v}(t)\dot{\boldsymbol{\mu}}^{\mathrm{T}}(0)\rangle$. Here $\mathbf{v}$ is the molecular center-of-mass linear velocity, $\boldsymbol{\omega}$ its angular velocity and $\boldsymbol{\mu}$ the net molecular dipole moment. These ccf's we reported here using computer simulation of liquid dichloromethane at 269K treated with a strong electric field [5], in the z axis of the laboratory frame, energetically equivalent to $\mu E/kT = 2.8$. They are also described analytically with a rigorous approximation of the stochastic Liouville equation developed by Grigoloni [6]. In well-defined limiting cases it is possible to anticipate liquid crystal type behaviour [7] based on the existence of these ccf's alone, without the use of a "director" potential. In the Markov limit [8], an equation is derived linking the cross-correlation function to the angular velocity (or rotational velocity) auto correlation functions (acf's) ‖ and ⊥ to the applied electric field. This equation shows that induced birefringence always results in the appearance of observable ccf's in the laboratory frame, whatever the strength of the applied electric field. This is an original result and provides a method for the experimental measurement of these new ccf's using conventional Kerr effect apparatus [1], preferably at far infrared-frequencies [7,8].

Analytical theory. A brief synopsis of the analytical results is given in this section. These are based on the stochastic Liouville equation [6]:

$$\dot{A}(t) = \mathcal{L}_0 A(t)\,, \tag{1}$$

where A is a column vector of variates [8], and $\hat{\mathcal{L}}_0$ the Liouville operator. If we want an expression for $C_{v\omega} = \langle \mathbf{v}(t)\boldsymbol{\omega}^{\mathrm{T}}(0)\rangle$ then:

$$A = \begin{bmatrix} \mathbf{v}(t) \\ \boldsymbol{\omega}(t) \end{bmatrix},$$

and similarly for $\langle \mathbf{v}(t)\dot{\boldsymbol{\mu}}^{\mathrm{T}}(0)\rangle$, or any other non-vanishing ccf. In the presence of an electric field $\langle \mathbf{v}(t)\boldsymbol{\omega}^{\mathrm{T}}(0)\rangle \neq 0$; $\langle \mathbf{v}(t)\dot{\boldsymbol{\mu}}^{\mathrm{T}}(0)\rangle \neq 0$. This is confirmed in this letter by computer simulation. [The accepted dynamical theory of induced birefringence assumes implicitly that these ccf's vanish for all t, i.e. uses $A \equiv \boldsymbol{\omega}(t)$.]

Using projection operators Grigolini et al. [9] have reduced eq. (1) to a form suitable for the calculation of correlation functions:

$$\dot{\mathbf{C}}(t) = \boldsymbol{\lambda}(t)\mathbf{C}(t) - \int_0^t (t-\tau)\mathbf{C}(\tau)\,\mathrm{d}\tau\,. \tag{2}$$

When considering the ccf between $\mathbf{v}$ and $\boldsymbol{\omega}$ we have:

$$\mathbf{C}(t) = \begin{bmatrix} \langle \mathbf{v}(t)\mathbf{v}^{\mathrm{T}}(0)\rangle & \langle \mathbf{v}(t)\boldsymbol{\omega}^{\mathrm{T}}(0)\rangle \\ \langle \boldsymbol{\omega}(t)\mathbf{v}^{\mathrm{T}}(0)\rangle & \langle \boldsymbol{\omega}(t)\boldsymbol{\omega}^{\mathrm{T}}(0)\rangle \end{bmatrix},$$

$$\boldsymbol{\lambda}(t) = \mathrm{i}\omega_1 \begin{bmatrix} \mathbf{0} & \mathbf{0} \\ \mathbf{0} & \mathbf{1} \end{bmatrix}, \quad \omega_1 = \mu E/I\,,$$

where I is the moment of inertia of the molecule, assumed for simplicity to be a spherical top. In the Markov limit:

$$\boldsymbol{\phi} = \begin{bmatrix} \boldsymbol{\phi}_{vv} & \boldsymbol{\phi}_{v\omega} \\ \boldsymbol{\phi}_{\omega v} & \boldsymbol{\phi}_{\omega\omega} \end{bmatrix},$$

where $\boldsymbol{\phi}_{vv}$, $\boldsymbol{\phi}_{v\omega} = \boldsymbol{\phi}_{\omega v}$ and $\boldsymbol{\phi}_{\omega\omega}$ are friction matrices. The matrices $\langle \mathbf{v}(t)\mathbf{v}^{\mathrm{T}}(0)\rangle$, $\langle \boldsymbol{\omega}(t)\boldsymbol{\omega}^{\mathrm{T}}(0)\rangle$, $\boldsymbol{\phi}_{vv}$ and $\boldsymbol{\phi}_{\omega\omega}$ are diagonal; and the matrices $\langle \mathbf{v}(t)\boldsymbol{\omega}^{\mathrm{T}}(0)\rangle = \langle \boldsymbol{\omega}(t)\mathbf{v}^{\mathrm{T}}(0)\rangle$, and $\boldsymbol{\phi}_{v\omega} = \boldsymbol{\phi}_{\omega v}$ are off-diagonal in structure, with elements in the x, y and z axes of the laboratory frame. For example, the computer simulation results show that, to a good approximation:

$$\mathbf{C}_{v\omega}(t) = \mathbf{C}_{\omega v}(t) = C^{xy}_{v\omega}(t) \begin{bmatrix} 0 & -1 & 0 \\ 1 & 0 & 0 \\ 0 & 0 & 0 \end{bmatrix}, \tag{3}$$

where $C^{xy}_{v\omega}(t)$ is an observable, scalar, ccf. Eq. (3) shows that the dominant elements of $C_{v\omega}(t)$ [fig. (1)] are the (y, x) and (x, y) elements, which are mirror images. By solving eq. (2) using Laplace transformation, and by comparing elements in the resulting supermatrix equation, a series of relations is obtained between the ccf $C^{xy}_{v\omega}(t)$ and the angular and linear velocity acf's in the x and z direction of the lab. frame. The most significant of these is, to a good approximation:

$$C^{xy}_{v\omega}(p) = \frac{\langle v_z^2\rangle}{\phi^{xy}_{v\omega}} \frac{C^{xx}_{vv}(p)}{C^{zz}_{vv}(p)} - \frac{\langle v_x^2\rangle}{\phi^{xy}_{v\omega}}$$

$$= \frac{\langle \omega_z^2\rangle}{\phi^{xy}_{v\omega}} \frac{C^{xx}_{\omega\omega}(p)}{C^{zz}_{\omega\omega}(p)} - \frac{\langle \omega_x^2\rangle}{\phi^{xy}_{v\omega}}\,. \tag{4}$$

Here, $C^{xy}_{v\omega}(p)$ is the Laplace transform of $C^{xy}_{v\omega}(t)$. $C^{xx}_{vv}(p)$ and $C^{zz}_{vv}(p)$ are Laplace transforms of the linear velocity acf ⊥ and ∥ to the electric field. $\langle v_x^2\rangle$ and $\langle v_z^2\rangle$ are the mean square velocities ⊥ and ∥ to the field. There are similar definitions for the angular velocity in eq. (4), where $\phi^{xy}_{v\omega}$ is the mixed friction coefficient. Note that eq. (4) implies that $C^{xy}_{v\omega}(t)$ vanishes in the absence of birefringence. The ccf's in eq. (4) are defined by

$$C^{xx}_{\omega\omega}(p) = D^{-1}\langle \omega_x^2\rangle (p + \phi^{xx}_{vv})\,, \tag{5}$$

$$C^{xx}_{vv}(p) = D^{-1}(v_x^2\rangle(p - \mathrm{i}\omega_1 + \phi^{xx}_{\omega\omega})\,, \tag{6}$$

$$C^{xy}_{v\omega}(p) - D^{-1}\langle \omega_x^2\rangle \phi^{xy}_{v\omega}\,, \tag{7}$$

$$D = (p + \phi^{xx}_{vv})\,(p - \mathrm{i}\omega_1 + \phi^{xx}_{\omega\omega}) + (\phi^{xy}_{v\omega})^2\,,$$

$$C^{zz}_{\omega\omega}(p) = \langle \omega_z^2\rangle/(p - \mathrm{i}\omega_1 + \phi^{zz}_{\omega\omega})\,, \tag{8}$$

$$C^{zz}_{vv}(p) = \langle v_z^2\rangle/(p + \phi^{zz}_{vv})\,. \tag{9}$$

Similar results can be obtained for $\langle \mathbf{v}(t)\,\dot{\boldsymbol{\mu}}^{\mathrm{T}}(0)\rangle$. The analytical results (the real parts of the inverse Laplace transforms of eqs. (5)–(9)) are compared with the computer simulations of the equivalent correlation functions in figs. (1)–(3).

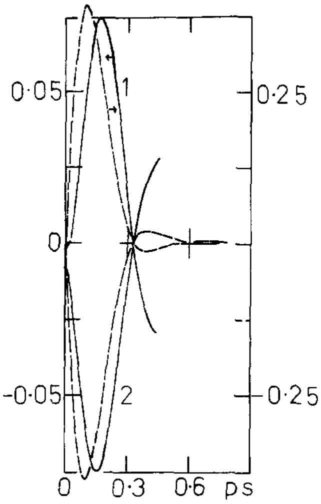

Fig. 1. Simulated and analytical: $C^{xy}_{v\omega}(t)$ and $C^{yx}_{v\omega}(t)$. —— (1) $C^{yx}_{v\omega}(t)$, simulated; – – – analytical theory (r.h. scale). (2) As for (1), $C^{xy}_{v\omega}(t)$. Ordinate: normalized ccf; abscissa: time/ps.

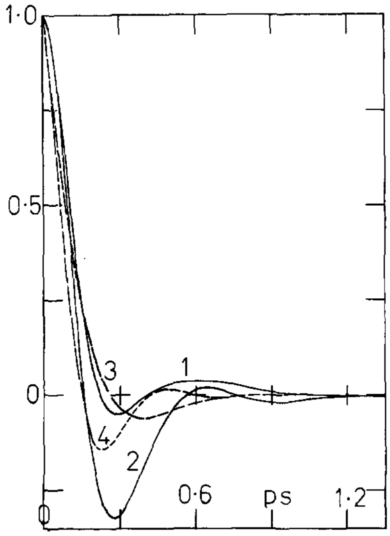

Fig. 2. —— (1) $\langle\omega_z(t)\omega_z(0)\rangle/\langle\omega_z^2\rangle$; (2) $\langle\omega_x(t)\omega_x(0)/\langle\omega_x^2\rangle$, the simulated angular velocity acf's ∥ and ⊥ to the electric field. – – – (3) and (4); As for (1) and (2) respectively, analytical theory. Ordinate: normalised acf; Abscissa: time/ps.

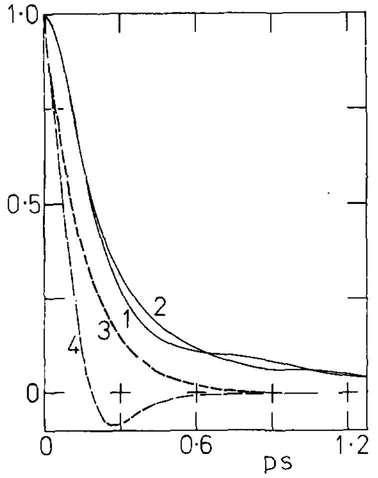

Fig. 3. As for fig. (2); linear, centre of mass, velocity acf's.

Results and discussion. Eq. (4) shows that the hitherto unmeasured ccf $C_{v\omega}^{xy}(t)$, up to now unrecognised in the theory of birefringence, can be observed with conventional or slightly modified, Kerr effect apparatus [1]. To check the analytical results a computer simulation of the appropriate correlation functions has been carried out on 108 CH_2Cl_2 molecules at 296 K in the liquid. The pair potential was modelled simply with 3 sites [5], and built up of 3 × 3 Lennard-Jones and partial charge interactions with the parameters: $\epsilon/k(\mathrm{Cl{-}Cl}) = 173.5$ K; $\epsilon/k(\mathrm{CH_2{-}CH_2}) = 70.5$ K; $\sigma(\mathrm{CH_2{-}CH_2}) = 3.96$ A; $\sigma(\mathrm{Cl{-}Cl}) = 3.35$ A; $q_{\mathrm{Cl}} = -0.15\,|e|$; $q_{\mathrm{CH_2}} = 0.30\,|e|$. An electric field was applied in the z axis exerting a torque $-\boldsymbol{\mu} \times E$ on each molecule. The acf's and ccf's of interest were then built up, over about 3000 time steps of 0.005 ps, using standard running-time algorithms [8]. The ccf's from the computer simulation (and theory) are normalised, e.g.

$$C_{v\omega}^{xy} = \langle v_x(t)\omega_y(0)\rangle/\langle v_x^2\rangle^{1/2}\langle\omega_y^2\rangle^{1/2} .$$

They should vanish at $t = 0$: if they do not then this is merely an indication of the statistical noise level in the computer simulation, e.g. fig. (1).

The analytical and simulated cf's were compared by fitting the simulated $C_{\omega\omega}^{zz}(t)$ giving $\phi_{\omega\omega}^{zz} = 6.4$ THz; $\omega_1 = 6.0$ THz. For simplicity it was then assumed that $\phi_{\omega\omega}^{zz} = \phi_{\omega\omega}^{xx} = \phi_{vv}^{zz} = \phi_{vv}^{xx}$; and the other cf's generated by varying $\phi_{v\omega}^{xy}$ only. Figs. (1)–(3) are for $\phi_{v\omega}^{xy} = 9.0$ THz. Both the analytical and simulated cf's in figs. (1)–(3) are produced self-consistently. For these parameters the analytical ccf's are greater in normalised intensity than the simulated ccf's (±0.35 cf. ± 0.07), and less oscillatory, (because of the Markov structure of $\boldsymbol{\phi}$). The birefringence in the simulated and analytical angular velocity acf's is in the same sense [fig. (2)], but this time the analytical result is the smaller in magnitude. In fig. (3) there is a small (but real) birefringence in the simulated linear velocity acf, which, as $t \to \infty$, is in the same sense but much smaller, this time, than the Markov analytical result.

Overall, therefore, both theory and simulation point clearly towards the way to measure $C_{v\omega}^{xy}(t)$ and $C_{v\omega}^{yx}(t)$. We note to finish that: (i) the analytical theory used here is the simplest possible (with no time dependence for $\boldsymbol{\phi}$), and can be improved with the methods of Grigolini et al. [10]. (ii) An entirely analogous theory can be constructed for $\langle\mathbf{v}(t)\dot{\boldsymbol{\mu}}(0)\rangle$. By computer simulation the only non-vanishing element is $\langle v_x(t)\dot{\mu}_z(0)\rangle$. In consequence, the birefringence in $\langle\dot{\boldsymbol{\mu}}(t)\cdot\dot{\boldsymbol{\mu}}(0)\rangle$ is opposite in sense to that in $\langle\boldsymbol{\omega}(t)\dot{\boldsymbol{\omega}}(0)\rangle$ for the same z axis electric field. This can be picked up directly and accurately using polarised probe carcinotrons as far as intra-red birefringence at different spot frequencies. (iii) In the limit ($\omega_1 \to 0$, $\phi_{v\omega}^{xy} \to \infty$)

the anisotropy in the acf's becomes very large, the situation, generally speaking, encountered in an aligned nematic condition [7]. (iv) There is a relation between ω_1 and $\phi_{v\omega}^{xy}$ because ω_1 must vanish when $\phi_{v\omega}^{xy}$ vanishes and vice versa. (v) It is possible to extend the simulations to the "experimental" limit $\mu E/kT \ll 1$ with the "difference technique" developed by Heyes [11].

The University of Wales is thanked for a Fellowship.

References

[1] M.S. Beevers and D.A. Elliott, Mol. Cryst. Liq. Cryst. 53 (1979) 111.

[2] W.D. Condiff and J.S. Dahler, J. Chem. Phys. 44 (1966) 3988.

[3] U. Steiger and R.F. Fox, J. Math. Phys. 23 (1982) 296.

[4] B.J. Berne and R. Pecora, Dynamic light scattering with reference to physics, chemistry and biology (Wiley/Interscience, New York, 1976).

[5] M.W. Evans, J. Chem. Phys. 76 (1982) 5473, 5480; 77 (1982) 4632; 78 (1983) 925, 5403.

[6] W.T. Coffey, M.W. Evans and P. Grigolini, Molecular diffusion (Wiley/Interscience, New York, 1984) ch. 7–9.

[7] M.W. Evans, G.J. Evans, W.T. Coffey and P. Grigolini, Molecular dynamics (Wiley/Interscience, New York, 1982) ch. 8.

[8] M.W. Evans, G.J. Evans, W.T. Coffey and P. Grigolini, Molecular dynamics (Wiley/Interscience, New York, 1982) ch. 1.

[9] M.W. Evans, G.J. Evans, W.T. Coffey and P. Grigolini, Molecular dynamics (Wiley/Interscience, New York, 1982) ch. 10.

[10] M.W. Evans, P. Grigolini and G. Pastori-Parravici, eds., Memory function approaches to stochastic problems in condensed matter, in: Advances in chemical physics, (Wiley/Interscience, New York, 1984).

[11] D. Heyes, S.E.R.C., CCP5 Quarterly Review, Daresbury Laboratory, Warrington, UK.